LILRB2/PirB mediates macrophage recruitment in fibrogenesis of nonalcoholic steatohepatitis

Yong Chen (tj.y.chen@vip.163.com)
Tongji Hospital, Tongji Medical College, Huazhong University of Science and Technology
https://orcid.org/0000-0002-3634-0328

xue yu
tongji medical school

Danpei Li

Li Huang
Tongji Hospital, Tongji Medical College, Huazhong University of Science and Technology

Xiao-Yu Meng
Tongji Hospital, Tongji Medical College, Huazhong University of Science and Technology

Shu-Yun Wang
Tongji Hospital, Tongji Medical College, Huazhong University of Science and Technology

Ran-Ran Kan
Tongji Hospital, Tongji Medical College, Huazhong University of Science and Technology

Hua-Jie Zou
Tongji Hospital, Tongji Medical College, Huazhong University of Science and Technology

Ya-Ming Guo
Tongji Hospital, Tongji Medical College, Huazhong University of Science and Technology

Li-Meng Pan
Tongji Hospital, Tongji Medical College, Huazhong University of Science and Technology

Pei-Qiong Luo
Tongji Hospital, Tongji Medical College, Huazhong University of Science and Technology

Yu-Xi Xiang
Tongji Hospital, Tongji Medical College, Huazhong University of Science and Technology

Bei-Bei Mao
Tongji Hospital, Tongji Medical College, Huazhong University of Science and Technology

Zhi-Han Wang
Tongji Hospital, Tongji Medical College, Huazhong University of Science and Technology

Rui He
Tongji Hospital, Tongji Medical College, Huazhong University of Science and Technology

Yan Yang
Tongji Hospital, Tongji Medical College, Huazhong University of Science and Technology

Zhelong Liu

Tongji Hospital, Tongji Medical College, Huazhong University of Science and Technology
Jun-Hui Xie
Tongji Hospital, Tongji Medical College, Huazhong University of Science and Technology
Delin Ma
Tongji Hospital, Tongji Medical College, Huazhong University of Science and Technology
Ben-Ping Zhang
Tongji Hospital, Tongji Medical College, Huazhong University of Science and Technology
Shi-Ying Shao
Tongji Hospital, Tongji Medical College, Huazhong University of Science and Technology
Xi Chen
Tongji Hospital, Tongji Medical College, Huazhong University of Science and Technology
Simiao Xu
Tongji Hospital, Tongji Medical College, Huazhong University of Science and Technology
Wen-Tao He
Tongji Hospital, Tongji Medical College, Huazhong University of Science and Technology
Wen-Jun Li
Tongji Hospital, Tongji Medical College, Huazhong University of Science and Technology

---

Article

Keywords: Nonalcoholic steatohepatitis, paired immunoglobulin-like receptor B, angiopoietin-like protein 8, macrophage, steatosis, inflammation, fibrosis

Posted Date: September 6th, 2022

DOI: https://doi.org/10.21203/rs.3.rs-1993483/v1

Version of Record: A version of this preprint was published at Nature Communications on July 22nd, 2023. See the published version at https://doi.org/10.1038/s41467-023-40183-3.

Abstract

Inhibition of immunocyte infiltration and activation has been proven to effectively ameliorate hepatic inflammation and fibrosis in nonalcoholic steatohepatitis (NASH). Paired immunoglobulin-like receptor B (PirB) and its human orthologue receptor, leukocyte immunoglobulin-like receptor B (LILRB2), are immune-inhibitory receptors with unknown roles in NASH. Here, we demonstrate that PirB/LILRB2 regulates the migration of macrophages in NASH pathogenesis and fibrogenesis by binding to its NASH-associated ligand angiopoietin-like protein 8 (ANGPTL8). Mechanistically, PirB facilitates the ANGPTL8-induced infiltration of monocyte-derived macrophages (MDMs) into the liver by regulating the phosphorylation of P38, AKT, and P65. Hepatocyte-specific knockout of its ligand ANGPTL8 reduces MDM infiltration and resolves lipid accumulation and fibrosis progression in the livers of NASH mice. In addition, $PirB^{-/-}$ bone marrow (BM) chimaeras abrogated ANGPTL8-induced MDM migration to the liver. PirB ectodomain protein can ameliorate the lipid accumulation inflammatory response and fibrosis of NASH by sequestering ANGPTL8. Furthermore, LILRB2-ANGPTL8-axis-associated MDM migration and inflammatory activation are also observed in human peripheral blood monocytes. Taken together, our findings reveal a novel role of PirB/LILRB2 in NASH pathogenesis and identify PirB/LILRB2-ANGPTL8 signalling as a potential target for the management or treatment of NASH.

Introduction

Nonalcoholic fatty liver disease (NAFLD), which is one of the most common liver disorders, is associated with increased overall mortality[1,2]. Nonalcoholic steatohepatitis (NASH), the inflammatory subtype of NAFLD, has a higher probability of progressing to end-stage liver diseases, such as cirrhosis and hepatic carcinoma[3]. However, there remain difficulties in the treatment of NASH due to a lack of approved pharmacological agents[2]. Therefore, it is urgent to identify novel targets for better implementation of NASH treatment.

Liver macrophages have been shown to be involved in the progression of steatohepatitis and subsequently hepatic fibrosis[4]. The liver harbours the largest proportion (approximately 80%) of macrophages in the body[5]. Liver macrophages consist of heterogeneous populations, including Kupffer cells (KCs), which are resident and principally nonmigratory phagocytes with self-renewing ability, and monocyte-derived macrophages (MDMs), which are recruited from circulation. The macrophage pool of the liver can be rapidly expanded by infiltrated MDMs when KCs are decreased during diseases or after injury[6]. Experimental mouse models of NASH have displayed increased MDM infiltration and cytokine release, which are critical pathogenic events promoting steatohepatitis and hepatic fibrogenesis[7]. Hence, inhibition of MDM recruitment and activation could be a widely accepted therapeutic strategy to attenuate steatohepatitis [7–10].

Paired immunoglobulin-like receptor B (PirB) and its human orthologue receptor, leukocyte immunoglobulin-like receptor B-2 (LILRB2), are mainly expressed in various immunocytes and enable

them to properly respond to extrinsic stimuli[11]. PirB/LILRB2 are classified as inhibitory receptors for their intracytoplasmic domain (ITIM motifs), which can recruit phosphatases SHP-1, SHP-2, or SHIP to negatively regulate cell activation[11], such as downregulation of immune responses and inhibition of regeneration of adult neuron cells[12]. However, the role of PirB in hepatic inflammation is unknown. Considering that the liver harbours many immunocytes and that the metabolic homeostasis of the whole body is maintained by hepatic immunologic balance, PirB/LILRB2, as an immune-inhibitory receptor, could play a pivotal role in metabolic diseases. Through analysing published RNA-seq data[13, 14], we found that LILRB2 expression in livers is increased in NAFLD/NASH patients. As immunosuppression has been proven to be effective for ameliorating hepatic inflammation and fibrosis in NASH [2], we speculated that LILRB2/PirB, as immune-inhibitory receptors, would be potential targets for NASH therapy.

LILRB2 has been proven to be a receptor for several angiopoietin-like proteins (ANGPTLs), and the binding of ANGPTLs to these receptors supported the ex vivo expansion of haematopoietic stem cells[15]. In contrast to other ANGPTLs, ANGPTL8 is a hepatokine that is exclusively expressed by the liver in humans[16]. More importantly, ANGPTL8 is associated with NAFLD both in mice and humans[17], albeit with unsolved mechanisms. Recent studies suggested that ANGPTL8 was a ligand for PirB[18, 19]. Whether ANGPTL8 interacts with PirB and acts as a pro- or anti-inflammatory factor and whether circulating ANGPTL8 exerts extracellular functions in metabolic diseases remain controversial [16, 20].

In this study, we explored the role of LILRB2/PirB and their NASH-associated ligand in steatohepatitis, providing evidence that the LILRB2/PirB-ANGPTL8 axis is the pathogenic driver of NASH pathogenesis and fibrogenesis.

Results

Hepatic LILRB2/PirB are increased in NASH patients and murine models

To investigate hepatic expression of LILRB2 in patients during NASH progression, RNA-seq analysis was performed using data published in the NCBI GEO repository [13, 14]. Liver samples from NASH patients were histologically scored from 0 (normal control) to 8 according to the semiquantitative NASH-Clinical Research Network NAFLD Activity Score [21]. LILRB2 mRNA expression was increased in the livers of simple steatosis and NASH patients (Fig. 1a-c). Meanwhile, the expression of its ligand ANGPTL8 in the liver was significantly higher in patients with the full spectrum of NASH (scored as 1–8) than in the controls (scored as 0) (Fig. 1d). In addition, we noticed that LILRB2 expression in the liver was even higher in NASH patients than in simple steatosis patients (Fig. 1b).

To test whether PirB and its ligand ANGPTL8 were upregulated in mice during NASH progression, we developed murine NASH models by feeding C57BL/6 mice a 6-month choline-deficient high-fat diet (CDHFD) or a 2-month methionine-choline deficient (MCD) diet (Fig. 1e-h). NASH was determined by

histological characterization of the liver (Fig. 1e) and auxiliarily by remarkable increases in the liver-to-body weight ratio, hepatic TG content, and abnormalities in liver functions (Fig. S1a-e). Compared with age-matched controls, livers of NASH models exhibited significantly elevated PirB and ANGPTL8 at both the transcriptional and translational levels (Fig. 1f-h).

Hepatic PirB is mainly expressed in monocyte-derived macrophages (MDMs)

PirB was highly expressed in the immune and haematopoietic systems (Fig. 2a). To generate a PirB-expressing atlas in the liver, we examined different cell types in liver tissue and found that PirB was mainly expressed in hepatic macrophages (Fig. 2b).

Since hepatic macrophages include liver-resident Kupffer cells (KCs) and foreign monocyte-derived macrophages (MDMs) infiltrating from circulation [22]. We thus FACS-purified KCs ($F4/80^{hi}CD11b^{lo}CLEC2^{hi}Ly6c^{-}$) and MDMs ($F4/80^{lo}CD11b^{hi}CLEC2^{lo}Ly6c^{+}$) prior to qPCR and immunocytochemical analysis. The results showed that PirB was highly expressed in MDMs compared to KCs and colocalized with its ligand ANGPTL8 on the cell membrane by means of immunohistology and immunoprecipitation (Fig. 2c). After recombinant ANGPTL8 protein treatment, MDMs, but not KCs or hepatocytes, exhibited significantly increased cytokine expression (Fig. 2d), suggesting that MDMs may be potential cells targeted by ANGPTL8 in the liver.

ANGPTL8 promotes MDM migration and activation

Different from other ligands for PirB, ANGPTL8 is a unique secreted protein that is mainly expressed in liver tissue (Fig. S2a) and associated with the NAFLD Activity Score (Fig. 1d). To identify the potential functions of ANGPTL8 in MDMs, we further analysed ANGPTL8-induced changes in the transcriptional profile of MDMs through mRNA sequencing (Fig. 2e). Pathway enrichment analysis revealed that upregulated pathways in MDMs after ANGPTL8 treatment were correlated with leukocyte chemotaxis and migration (Fig. 2e). Furthermore, to understand the role of hepatocellular ANGPTL8 in liver macrophages, we generated mice with hepatocyte-specific *Angptl8* knockout (hereafter referred to as $Angptl8^{HepKO}$) (Fig. S2a). KO was determined by significantly decreased hepatic expression of ANGPTL8 (Fig. S2a). Although we failed to observe a difference in KC numbers between $Angptl8^{HepKO}$ and their *loxp/loxp* littermates (hereafter referred to as *loxp*) mice, we noticed that the $Angptl8^{HepKO}$ mice exhibited significantly decreased numbers of MDMs and Ly6C+ monocytes in the liver (Fig. 2f; Fig. S2b). Several previous studies have revealed that the depletion of KCs may result in compensatory generation of MDMs[23]. Nevertheless, in our study, KC depletion by clodronate liposomes led to an increase in MDM numbers only in the liver of the *loxp* mice but not in the $Angptl8^{HepKO}$ mice (Fig. 2g). In addition, no significant proliferative difference between MDMs and KCs was detected after administration of ANGPTL8 in vitro (Fig. S2c). Therefore, we speculated that $Angptl8^{HepKO}$ mice exhibited a reduced capacity for MDM recruitment and that ANGPTL8 may be required for MDMs to fill the empty niche that KCs vacated. This result was in agreement with the observed correlation between ANGPTL8 and leukocyte chemotaxis in pathway enrichment analysis (Fig. 2e).

To trace the origin of the increased MDMs after KC depletion, we first developed bone marrow (BM) chimaeras by transplanting 5×10^6 BM cells from congenic mTmG mice into *loxp* or *Angptl8*^{HepKO} recipient mice, which were exposed to low-dose irradiation (3 Gy) (Fig. 2h). We reasoned that such a mild irradiation regimen would be sufficient to favour the engraftment of donor cells, which will then generate and enable the tdTomato+ monocytes to enter the bloodstream and spare radioresistant KCs according to previous studies [23]. Not surprisingly, we examined the chimaerism of circulating monocytes 2 weeks after BM transplantation and found that more than 70% of the Ly-6C+ monocytes (FACS-purified) were tdTomato+ (Fig. S2d). Meanwhile, approximately 10% of the neutrophils and B cells and less than 2% of the T cells were tdTomato+ (Fig. S2d). These chimaeras were then injected with clodronate liposomes for 10 days. As expected, tdTomato+ cells were significantly increased in the livers of *loxp* mice, suggesting recruitment of these cells from the circulation after KC depletion. However, a minor change in tdTomato+ cells in the liver was observed in *Angptl8*^{HepKO} mice (Fig. 2i). To validate the contribution of ANGPTL8 to the liver MDM pool, different amounts of recombinant ANGPTL8 protein were injected into *Angptl8*^{HepKO} mice through the tail vein. MDM levels were increased 4-6 hours after rANGPTL8 injection in a dose-dependent manner (Fig. 2j). In vitro, MDMs were found to be transferred to the lower wells with recombinant ANGPTL8 protein treatment in a dose-dependent and time-responsive manner through a Transwell assay (Fig. 2k; Fig. S2e-f).

Moreover, we analysed the transcriptional changes in MDMs after ANGPTL8 treatment in vitro and found that M1 (inflammatory phenotype) marker genes were highly upregulated, whereas most M2 (anti-inflammatory phenotype) marker genes were downregulated or remained unchanged (Fig. S2g). Consequently, we referred to CD11c as an M1 marker and CD206 as an M2 marker with F4/80 costaining to identify the polarization of MDMs by flow cytometry. After ANGPTL8 treatment, the $CD11c^+$ population was increased (5.9% vs. 32.1%), whereas the $CD206^+$ population was decreased (69.5% vs. 27.4%) (Fig. 2l). This population shift was similar to the lipopolysaccharide (LPS)-induced shift in MDMs (Fig. 2l). These results implied that ANGPTL8-treated MDMs bore more resemblance to M1-like macrophages.

Considering that M1 macrophages and their derived proinflammatory cytokines may regulate hepatocyte steatosis and apoptosis [24-26], we cocultured primary hepatocytes with MDMs to explore whether crosstalk exists between these two cell types (Fig. 2M). ANGPTL8 treatment in the coculture resulted in a significant increase in the levels of certain proinflammatory cytokines, including IL-1β, IL-6, and TNF-α, in the culture medium (Fig. S2h), an aggravation of hepatocyte apoptosis, a promotion of palmitate (PA)-induced formation of intracellular lipid vacuoles and an increase in TG content (Fig. 2m; Fig. S2i), and correspondingly, an upregulation of various lipogenic genes, including *Fasn*, *Srebp*, and *Scd-1* (Fig. S2j). However, primary hepatocytes from either *loxp* or *Angptl8*^{HepKO} mice (without MDM coculture) did not show any difference in PA-induced lipogenesis (Fig. S2k). These results indicated that macrophages were required for the effects of ANGPTL8 on hepatocytes.

ANGPTL8 activates NF-κB signalling through PirB

NF-κB is a key transcription factor implicated in the inflammatory signalling cascade of macrophages. A previous study suggested that ANGPTL8 is a negative regulator of NF-κB[27]. In contrast, our study observed an increase in the translocation of the P65 subunit of NF-κB to the nucleus in MDMs stimulated with rANGPTL8 (Fig. 3a). Consistently, an increase in the phosphorylation of the P65 subunit of NF-κB was also detected after rANGPTL8 treatment in a time-dependent manner (Fig. 3b). These data indicated that ANGPTL8 promotes the activation of NF-κB in MDMs. To elucidate the regulatory mechanisms through which ANGPTL8 enhances NF-κB activation, we tested the phosphorylation of various key upstream signalling molecules of NF-κB (including JAK1-STAT1, STAT6, P38, ERK1/2, AKT, IRAK-1 and TAK-1) and found that ERK1/2, P38, and AKT phosphorylation was also enhanced by rANGPTL8 treatment in MDMs (Fig. 3b left). These three molecules are downstream signalling factors of PirB [11, 18]. Furthermore, a neutralizing antibody for PirB ectodomains abrogated ANGPTL8-induced phosphorylation of P65, ERK1/2, P38, and AKT in MDMs (Fig. 3b right), indicating that ANGPTL8 may activate NF-κB through PirB.

PirB mediates ANGPTL8-induced MDM migration and activation

We next examined whether PirB mediates the effect of ANGPTL8 on MDM migration and activation. PirB antibodies also inhibited ANGPTL8-induced mRNA expression of certain proinflammatory cytokines (Fig. 3c). Importantly, blockade of TNF-α and PirB, but not IL-1b or IL-6, using corresponding neutralizing antibodies in coculture medium (hepatocytes cocultured with MDMs) protected hepatocytes from lipid accumulation and apoptosis (Fig. 3d). In addition, we purified MDMs using FACS from $PirB^{-/-}$ mice. Although slightly higher in expression, mRNA expression of cytokines (*Il-1b*, *Il-6*, and *Tnf-α*) in MDMs from $PirB^{-/-}$ mice showed no significant change after ANGPTL8 stimulation (Fig. 3e). Similar conclusions in migration were drawn when blocking or depleting PirB on MDMs (Fig. 3f-g). Blockade of PirB on MDMs from WT mice with anti-PirB ectodomain antibodies significantly reduced ANGPTL8-induced migration of MDMs (Fig. 3f). Likewise, MDMs from $PirB^{-/-}$ mice exhibited a lower response to ANGPTL8 stimulation in cell migration than those from WT mice (Fig. 3g). In addition to ANGPTL8, ANGPTL2 has also been proven to be associated with macrophage migration via integrin-α5β1 in adipose tissues[28]. However, in our study, ANGPTL8-induced migration of macrophages was independent of integrin-α5β1 receptors (Fig. 3f), possibly because of the absence of a fibrinogen-like domain (which is contained in the other seven ANGPTL members) in the ANGPTL8 protein structure[29]. Considering that the amino acid sequences of PirB ectodomains are highly homologous with those of PirAs (over 92% identity) and that both receptors contain six extracellular immunoglobulin-like domains [11], we also validated whether PirA contributes to ANGPTL8-induced MDM activation. Knockdown of PirA in RAW264.7 cells through lentiviral shRNA did not result in an inhibition in ANGPTL8-induced expression of the cytokines, while knockdown of PirB impaired the dose-dependent upregulation of *Il-1β*, *Il-6*, and *Tnf-α* by ANGPTL8 (Fig. S3a-b), suggesting that PirB but not PirA receptors mediates the above effects of ANGPTL8. Moreover, we observed that the inhibition of three main downstream signalling molecules of PirB (P38, AKT and NF-κB) through their corresponding inhibitors (SB203580, MK-2206, and BAY 11-7082) led to an abrogation in ANGPTL8-

induced MDM activation and migration, whereas an ERK1/2 inhibitor (U0126) alone failed to have a similar effect (Fig. S3c-e).

To further understand PirB function in vivo, we generated BM chimaeras by irradiating *loxp* and *Angptl8*^{HepKO} mice and reconstituted them with BM from WT or *PirB*$^{-/-}$ mice, respectively (WT/*PirB*$^{-/-}$→loxp; WT/PirB$^{-/-}$→*Angptl8*^{HepKO}) (Fig. 3h). Compared with the control (WT→*loxp*), MDM recruitment was significantly reduced in the liver of *loxp*-based *PirB*$^{-/-}$ BM chimaeras (PirB$^{-/-}$→*loxp*) 10 days after clodronate liposome administration. In contrast, *Angptl8*^{HepKO}-based *PirB*$^{-/-}$ BM chimaeras (PirB$^{-/-}$→*Angptl8*^{HepKO}) maintained the same friction of recruited MDMs as *Angptl8*^{HepKO}-based WT BM chimaeras (Fig. 3i). Taken together, our data show that PirB mediates the effects of ANGPTL8 on MDM migration and activation both in vitro and in vivo.

MDM depletion reduced inflammation and fibrosis in NASH

Our previous data revealed that the macrophages (MDMs) that accumulated in the liver of NASH mice mainly originated from the bone marrow. To elucidate the role of MDMs in NASH, mice were fed a CDHFD for 6 months and received an injection of clodronate liposomes in the last month to deplete the macrophages (Fig. 4a, b). Macrophage depletion caused a 72.1% decrease in collagen fibres and a 53.4% decrease in lipid accumulation (Fig. 4c), concomitant with a 50% decrease in liver TG content and a 44.0% decrease in ALT plasma levels (Fig. 4e). These results indicated that MDM depletion protects mice from the development of steatohepatitis.

Hepatocyte-specific ANGPTL8 knockout reduces MDM infiltration into the liver and ameliorates NASH

As ANGPTL8 promoted macrophage migration to the liver according to our previous data, we wondered whether a reduction in hepatic ANGPTL8 could inhibit the development of CDHFD-induced NASH. *Angptl8*^{HepKO} mice together with their *loxp* littermates (as controls) were fed a CDHFD for 6 months (Fig. 4f). ANGPTL8 KO was determined by a significant decrease in hepatic expression of ANGPTL8 (Fig. S4a). *Angptl8*^{HepKO} mice exhibited a lower liver weight and liver/body weight ratio than the controls after 6 months of CDHFD (Fig. S4b). Importantly, specific *Angptl8* knockout in hepatocytes substantially attenuated hepatic lipid accumulation (evidenced by Oil Red O staining and liver TG content) (Fig. 4g, h), MDM recruitment (by CD11b staining and FACS) (Fig. 4g and Fig. S4c, d) and presented less accumulation of extracellular matrix (by Sirius Red staining) (Fig. 4g). Plasma ALT levels were also improved in *Angptl8*^{HepKO} mice (Fig. 4i). Moreover, *Angptl8* deficiency in hepatocytes attenuated the CDHFD-induced increase in inflammatory marker expression (including *Il-1β*, *Il-6*, *Tnf-α*, and *Tgf-β*) (Fig. 2j). In summary, hepatocyte-specific ANGPTL8 knockout prevented CDHFD-induced hepatic inflammation and fibrosis.

Soluble PirB ectodomain (sPirB) attenuated NASH

Soluble ectodomains of receptors act as decoys to sequester endogenous ligands, which could result in a reduction in ligand binding and subsequent receptor signalling. Soluble PirB ectodomain protein (sPirB)

has been thought to be a potential therapeutic approach for neurological diseases[30, 31]. However, the effect of sPirB on NASH has not yet been reported. To study this, we generated a sPirB containing the first six immunoglobulin G (Ig)–like domains and His tags for its further purification and detection (Fig. S4e). To determine the harbouring ability of sPirB, the protein levels of sPirB in the liver were evaluated. Twenty-four hours after sPirB injection through the tail vein, there was an increased level of $(His)_6$-positive proteins in the liver when the sPirB administration amount reached 1 mg/kg or 3.0 mg/kg (Fig. S4f). The sPirB protein expression level was increased 12 h after 1 mg/kg sPirB injection, peaked at 24 h and persisted for 72 h (Fig. S4f). Therefore, we injected CDHFD-fed control and *Angptl8*^{HepKO} mice with 1 mg/kg sPirB once every three days (Fig. 4k). After 3 months of injection, the fractions of MDMs in control mice, but not in *Angptl8*^{HepKO} mice, were significantly decreased (Fig. 4l). Moreover, sPirB administration resulted in a reduction in collagen fibres and hepatocyte apoptosis in the livers of the control mice (Fig. 4m), whereas no obvious improvement was observed in *Angptl8*^{HepKO} mice (Fig. 4m) due to the slightly pathological basal liver histology of *Angptl8*^{HepKO} mice. These results suggest that sPirB could be a potential therapeutic agent for NASH.

LILRB2 mediates ANGPTL8-induced human peripheral blood monocyte migration

To evaluate the effects of ANGPTL8 and LILRB2 on circulating monocytes in humans, we collected peripheral blood monocytes from healthy adults and NAFLD patients. We found that ANGPTL8 colocalized with LILRB2 in circulating monocytes from healthy humans (Fig. 5a). Interestingly, we noticed that monocytes in NAFLD patients had higher LILRB2 expression than those in healthy individuals (Fig. 5b). Moreover, ANGPTL8-induced migration of circulating monocytes was more significant in NAFLD patients than in healthy people, and both could be abrogated by a neutralizing antibody against LILRB2 (Fig. 5c), indicating that LILRB2 may mediate ANGPTL8-induced monocyte migration. Similar to the results observed in mice, we also identified a proinflammatory effect of ANGPTL8 on monocyte-derived macrophages with increased mRNA expression of IL-1β, IL-6, and TNF-α after ANGPTL8 treatment (Fig. 5d), and this proinflammatory effect was also abrogated by a neutralizing antibody against LILRB2 (Fig. 5d). Moreover, we observed an indirect promotive function of ANGPTL8 in hepatocyte lipogenesis, which also involves hepatocyte-macrophage crosstalk in humans (Fig. 5f). These data further indicated that the ANGPTL8-LILRB2 axis could be a potential therapeutic target for NASH in humans.

Discussion

In our study, we identified PirB/LILRB2 on hepatic macrophages, which bind with their NASH-associated ligand (ANGPTL8) to trigger the recruitment of macrophages to the liver during NASH pathogenesis. In addition, the PirB/LILRB2-ANGPTL8 axis induces the proinflammatory phenotype and stimulates cytokine production in the liver via activation of the P38, AKT, and NF-κB signalling pathways, which in turn causes aggravation of hepatocyte lipid accumulation and exacerbation from simple steatosis to steatohepatitis.

It has long been demonstrated that MDM recruitment is a critical pathogenic event that promotes steatohepatitis and subsequently hepatic fibrosis in NASH[4, 7, 8, 32]. NASH mice display a much higher

number of recruited MDMs than resident KCs in the liver[23, 32], and hepatic inflammation during NASH is mainly induced by recruited MDMs rather than resident KCs[32, 33]. Depletion of MDMs protects mice from diet-induced hepatic steatosis and ameliorates the progression of NASH[26, 34, 35]. Therefore, MDM recruitment in the liver is now targeted for NASH treatment. In our study, we found that liver-specific ablation of *Angptl8* reduced MDM recruitment and lipid accumulation and attenuated fibrosis in the liver of a NASH murine model. In contrast to other chemokines (such as CCL2, CCL5 and CXCL10), which are expressed in various tissues and were previously reported to be associated with NASH[36–38], ANGPTL8 is exclusively secreted from the liver in humans[39], with largely unknown regulatory mechanisms in MDM migration even in NASH. Thus, hepatic ANGPTL8 could be a new target to benefit inflammation and fibrosis of the liver.

More importantly, in our study, we identified LILRB2/PirB as a new chemokine receptor on MDMs that mediates macrophage migration to the liver. The observations of ANGPTL8 raise another question: how does a secreted protein from the liver exert its effects on MDMs? This question implies us to the receptors on macrophages. Although several studies have already shown that ANGPTL8 physically interacts with PirB in cardiac progenitor cells or hepatoma cells in mice [18, 19], our subsequent experiments demonstrated that PirB receptors are mainly expressed in macrophages other than hepatocytes in the liver. We noticed that $PirB^{-/-}$-BM chimaeras exhibited decreased MDM infiltration in WT-based mice but did not influence $Angptl8^{HepKO}$-based mice (probably due to their lower basal MDM numbers), revealing that PirB plays a pivotal role in ANGPTL8-induced macrophage recruitment in livers. In addition, administration of the soluble form of the PirB ectodomain protein also attenuated MDM recruitment in the liver and restrained CDHFD-induced NASH by sequestering its ligand, ANGPTL8, suggesting that the PirB ectodomain protein could be a potential therapeutic agent for the treatment of NASH by competing with certain deleterious ligands.

Previous studies in NASH patients suggest that the accumulation and inflammatory polarization (M1-like) of hepatic macrophages is a hallmark feature of disease progression[40], and M1-like macrophages have been shown to be involved in the mechanisms of hepatocyte lipid metabolism[41, 42]. In our study, we found that ANGPTL8 oriented macrophages into an inflammatory phenotype, which is consistent with the increasing evidence supporting that ANGPTL8 functions as a proinflammatory protein[43–45]. In vitro, when cocultured with ANGPTL8-treated macrophages, hepatocytes exhibited increased lipid accumulation, elevated lipogenic genes, and aggravated apoptosis. These results are consistent with the observation that hepatocytes exhibited increased lipogenesis and apoptosis when cocultured with M1 macrophages in other studies [24–26]. In our study, we further showed that the proinflammatory effects of ANGPTL8 in the liver were mainly regulated although its interaction with PirB, as evidenced by abolished cytokine expression in $PirB^{-/-}$ macrophages or reduced cytokine expression in WT macrophages after treatment with neutralizing antibodies against PirB. Therefore, we consider PirB to be an important immune-inhibiting receptor that can be suppressed by its ligand, ANGPTL8, during NASH pathogenesis.

To understand the molecular mechanisms, it is necessary to elucidate the signalling pathways by which the ANGPTL8-PirB axis regulates cytokine production and MDM migration in the liver. Previous studies have shown that the activation of the transcription factor NF-κB is intensively involved in macrophage activation and is known to be central to the inflammatory aspects of NASH [11, 18, 46]. We thus examined NF-κB signalling and found that ANGPTL8 activated NF-κB in MDMs by translocating its P65 subunit to the nucleus. Furthermore, examination of the main upstream signalling pathways of NF-κB in MDMs found that only ERK1/2, P38, and AKT robustly responded to ANGPTL8 stimulation. PirB blockade with neutralizing antibodies or PirB knockdown through lentiviral infection abrogated the effects of ANGPTL8-induced phosphorylation of ERK1/2, P38, and AKT, suggesting that ANGPTL8-responsive signals are downstream of PirB. This result is consistent with previous studies showing that PirB regulates the phosphorylation of ERK1/2, P38, and AKT[11, 18]. Despite 92% identity with PirB ectodomains, PirA knockdown failed to have the same effect as the absence of immunoreceptor tyrosine-based inhibitory motif (ITIM)-like motifs in their cytoplasmic sequences on mediating signal transduction[11]. Taken together, ANGPTL8 induces the phosphorylation of ERK1/2, P38, AKT, and NF-κB signalling pathways through PirB receptors and activates hepatic macrophages by enhancing their proinflammatory effects and migration.

In summary, ANGPTL8-PirB/LILRB2 is an important signalling axis for NASH pathogenesis via crosstalk between hepatocytes and macrophages. It is possible that an increased ANGPTL8 level in the NASH liver results in an induction of hepatic macrophage polarization, an enhancement in proinflammatory cytokine production, and an increase in the recruitment of circulating monocytes/macrophages in the liver. Thus, blocking the binding of ANGPTL8 to PirB/LILRB2 receptors could be a promising therapeutic approach for the treatment of NASH. A better understanding of the biological function of the ANGPTL8-PirB/LILRB2 axis in inflammation would lead to a more profitable development of possible therapeutic agents for NASH treatment. Collectively, we revealed a previously unappreciated role of PirB/LILRB2 in NASH pathogenesis and identified ANGPTL8-PirB-NF-κB signalling as a potential target for the management of NASH in the future.

Methods

Mouse strains used in the study

Wild-type C57BL/6J mice were from Beijing Huafukang Bioscience Co., Ltd. (Beijing, China). Hepatocyte-specific *Angptl8*-knockout (*Angptl8*^{HepKO}) mice were generated by Cyagen Biosciences Inc. (Guangzhou, China, details listed in the Supplementary Methods). PirB knockout and mTmG mice were purchased from Cyagen Biosciences Inc. The animal housing and diets used are listed in the Supplementary Methods.

Liver macrophage depletion

Macrophage depletion was achieved by intraperitoneal injection of liposomes containing clodronate or PBS (5 mg/ml, 100 μl per 10 g mouse, Yeasen Biotechnology Co., Ltd., Shanghai, China). Mice with NASH

received an intraperitoneal injection of clodronate liposomes once a week in the last month of the diet intervention (CDHFD).

Total body irradiation and bone marrow transplantation

Loxp and *Angptl8*^{HepKO} mice were exposed to 3 Gy total body irradiation. Bone marrow cells were harvested from donor mice by gently flushing their femurs, and 5×10^6 cells were intravenously injected into each recipient mouse. A two-week recovery period was observed to ensure donor bone marrow engraftment and blood monocyte reconstitution.

Flow cytometry

Cell suspensions were stained with appropriate antibodies for 30 min on ice. The commercial antibodies used in this study included anti-mouse FITC-CD45 (BioLegend, CA, USA, #103108), BV421-F4/80 (BioLegend, CA, USA, #123137), Percp/Cy5.5-CD11b (BioLegend, CA, USA, #550993), APC-Ly6C (BioLegend, CA, USA, #), APC-Ly6G/Ly-6C (Gr-1) (BioLegend, CA, USA, #108411), PerCP-CD19 (BioLegend, CA, USA, #115531), APC-CD3 (BioLegend, CA, USA, #100235), APC-CD206 (BioLegend, CA, USA, #141707), and FITC-CD11c BioLegend, CA, USA, #117305). All antibodies were diluted according to the manual from the manufacturer's website. Dead cells and doublets were removed by dead-cell dye staining (Zombie Aqua Fixable Viability Kit, BioLegend, CA, USA, #B297827).

Coculture of hepatocytes and monocyte-derived macrophages (MDMs)

Primary hepatocytes (5×10^5) were seeded in the lower chamber of 24-well Transwell plates (Corning, NY, USA, #3450) 24 h before 2×10^5 primary mouse MDMs (isolation and differentiation described in the ***Supplementary Methods***) were seeded in the upper chamber. Half an hour later, the hepatocytes and MDMs were incubated with or without 250 μM palmitate (PA) (Kunchuang Biotechnology, Xian, China, #KCKJ008) and/or 40 nM recombinant ANGPTL8 (rANGPTL8) (Cusabio Biotechnology Co., Ltd., Wuhan, China, #CSB-MP844436MO) at 37 °C for 18 h. For neutralizing antibody experiments, anti-TNFα (Thermo Fisher Scientific, MA, USA, #AMC3012), anti-IL-1β (Thermo Fisher Scientific, MA, USA, #16-7012-81) and anti-IL-6 (Thermo Fisher Scientific, MA, USA, #16-7061-81) were present at 1 μg/ml, and anti-PirB was present at 10 μg/ml. After incubation, media and cells were collected for analysis of triglyceride (TG) accumulation and inflammatory cytokine production. The mRNA expression of cytokines in the hepatocytes (the lower plates) and MDMs (the upper wells) was detected.

Transwell migration assay

Primary mouse MDMs (5×10^5) were seeded with 100 μl of serum-free Dulbecco's modified Eagle medium (DMEM) atop 8-μm polycarbonate filter inserts in Transwell chamber plates (Corning, NY, USA, #3422), and 500 μl of serum-free DMEM was added to the lower chamber. After incubation for 30 min, PBS or 5 nM, 20 nM, or 40 nM rANGPTL8 protein was added to the lower chamber. After incubation for 6 h, 12 h or 24 h, cells that had not migrated were removed with

a cotton swab from the upper surface of filters, and cells that had migrated to the lower surface of the membrane were stained with crystal violet at 25°C for 10 min, washed with PBS, and subsequently observed with a light microscope.

PirB ectodomain protein injection

The recombinant protein for PirB (sPirB) was prepared by Cusabio (Wuhan, China, # CSB-MP012941MO2). The PirB ectodomain DNA fragment was synthesized by CUSABIO (Wuhan, China). The DNA fragment was inserted into the pSecTag2A plasmid, which contained a $(His)_6$ tag. The plasmid was transformed into HEK293 cells, and the recombinant protein was purified using a Ni^{2+}-nitrilotriacetic acid super flow agarose column. CDHFD-fed *loxp* and *Angptl8*^{HepKO} mice received an intravenous injection of 1 mg/kg sPirB once every three days for three months.

Human peripheral blood and liver samples

Heparinized blood samples obtained from the Tongji Hospital of Wuhan were collected from NAFLD patients (n = 11, from the endocrinology department) and healthy volunteers (n = 10, from the physical examination centre). Primary liver specimens (n = 9) were obtained from haemangioma surgical resection. The isolation of human primary liver cells and human peripheral blood monocytes is listed in the ***Supplementary Methods.***

Statistical analyses

For animal studies, mice were randomized by body weight prior to dietary challenge, and no blinding was performed for subsequent analyses. Statistical analyses were performed with Prism 7 (GraphPad Software, Inc., USA) or RStudio version 1.1.442 (RStudio, Inc., USA). For data with a normal distribution and homogeneity of variance, one-way ANOVA was performed for comparisons among more than two groups. Two-tailed Student's t tests were performed to evaluate significant differences between two groups. The statistical tests used for each experiment are indicated in the figure legends. All data are expressed as the mean ± s.e.m. unless otherwise indicated. Differences for which $P < 0.05$ were considered significant. All in vitro experiments were performed in triplicate. Animal feeding, treatments and histological analyses were performed in a single-blinded fashion. No blinding was used for the remaining analyses.

Details of the isolation of primary cells, immunocytochemistry, oil red O staining, RNA sequencing (RNA-seq), real-time quantitative PCR (qPCR), western blotting and other experiments are provided in the ***Supplemental Methods***.

Data availability statements

All methods and protocols used are included in the main manuscript or supplementary files. All reagents, antibodies, and resources are listed in the Supplementary tables.

Declarations

Ethics: For all human studies in “LILRB2/PirB mediates macrophage recruitment in fibrogenesis of nonalcoholic steatohepatitis”, the Ethical approval was granted from the Medical Ethics Committee of the Tongji Hospital, Tongji Medical College, Huazhong University of Science and Technology, and all studies were performed in accordance with the Declaration of Helsinki. The study was explained in detail to each participant and informed written consent was obtained.

References

1. Sheka AC, Adeyi O, Thompson J, Hameed B, Crawford PA, Ikramuddin S. Nonalcoholic Steatohepatitis: A Review. JAMA **323**, 1175–1183 (2020).
2. Roeb E, Geier A. Nonalcoholic steatohepatitis (NASH) - current treatment recommendations and future developments. Z Gastroenterol **57**, 508–517 (2019).
3. Suzuki A, Diehl AM. Nonalcoholic Steatohepatitis. Annu Rev Med **68**, 85–98 (2017).
4. Parthasarathy G, Revelo X, Malhi H. Pathogenesis of Nonalcoholic Steatohepatitis: An Overview. Hepatol Commun **4**, 478–492 (2020).
5. Ju C, Tacke F. Hepatic macrophages in homeostasis and liver diseases: from pathogenesis to novel therapeutic strategies. Cell Mol Immunol **13**, 316–327 (2016).
6. Tacke F, Zimmermann HW. Macrophage heterogeneity in liver injury and fibrosis. Journal of Hepatology **60**, 1090–1096 (2014).
7. Tacke F. Targeting hepatic macrophages to treat liver diseases. J Hepatol **66**, 1300–1312 (2017).
8. Krenkel O, *et al.* Therapeutic inhibition of inflammatory monocyte recruitment reduces steatohepatitis and liver fibrosis. Hepatology **67**, 1270–1283 (2018).
9. Diaz Soto MP, Lim JK. Evaluating the Therapeutic Potential of Cenicriviroc in the Treatment of Nonalcoholic Steatohepatitis with Fibrosis: A Brief Report on Emerging Data. Hepat Med **12**, 115–123 (2020).
10. Baeck C, *et al.* Pharmacological inhibition of the chemokine CCL2 (MCP-1) diminishes liver macrophage infiltration and steatohepatitis in chronic hepatic injury. Gut **61**, 416–426 (2012).
11. Takai T. Paired immunoglobulin-like receptors and their MHC class I recognition. Immunology **115**, 433–440 (2005).
12. Takeda K, Nakamura A. Regulation of immune and neural function via leukocyte Ig-like receptors. J Biochem **162**, 73–80 (2017).
13. Ramachandran P, *et al.* Resolving the fibrotic niche of human liver cirrhosis at single-cell level. Nature **575**, 512–518 (2019).
14. Govaere O, *et al.* Transcriptomic profiling across the nonalcoholic fatty liver disease spectrum reveals gene signatures for steatohepatitis and fibrosis. Sci Transl Med **12**, (2020).

15. Zheng J, *et al.* Inhibitory receptors bind ANGPTLs and support blood stem cells and leukaemia development. Nature **485**, 656–660 (2012).
16. Abu-Farha M, Ghosh A, Al-Khairi I, Madiraju SRM, Abubaker J, Prentki M. The multi-faces of Angptl8 in health and disease: Novel functions beyond lipoprotein lipase modulation. Prog Lipid Res **80**, 101067 (2020).
17. Lee YH, *et al.* Association between betatrophin/ANGPTL8 and non-alcoholic fatty liver disease: animal and human studies. Sci Rep **6**, 24013 (2016).
18. Chen S, *et al.* Angptl8 mediates food-driven resetting of hepatic circadian clock in mice. Nat Commun **10**, 3518 (2019).
19. Chen S, *et al.* ANGPTL8 reverses established adriamycin cardiomyopathy by stimulating adult cardiac progenitor cells. Oncotarget **7**, 80391–80403 (2016).
20. Yang J, *et al.* Emerging roles of angiopoietin-like proteins in inflammation: Mechanisms and potential as pharmacological targets. J Cell Physiol, (2021).
21. Kleiner DE, *et al.* Design and validation of a histological scoring system for nonalcoholic fatty liver disease. Hepatology **41**, 1313–1321 (2005).
22. Krenkel O, Tacke F. Liver macrophages in tissue homeostasis and disease. Nat Rev Immunol **17**, 306–321 (2017).
23. Tran S, *et al.* Impaired Kupffer Cell Self-Renewal Alters the Liver Response to Lipid Overload during Non-alcoholic Steatohepatitis. Immunity **53**, 627–640 e625 (2020).
24. Park EJ, *et al.* Dietary and Genetic Obesity Promote Liver Inflammation and Tumorigenesis by Enhancing IL-6 and TNF Expression. Cell **140**, 197–208 (2010).
25. Ezquerro S, *et al.* Ghrelin Reduces TNF-alpha-Induced Human Hepatocyte Apoptosis, Autophagy, and Pyroptosis: Role in Obesity-Associated NAFLD. J Clin Endocrinol Metab **104**, 21–37 (2019).
26. Huang W, *et al.* Depletion of liver Kupffer cells prevents the development of diet-induced hepatic steatosis and insulin resistance. Diabetes **59**, 347–357 (2010).
27. Zhang Y, *et al.* ANGPTL8 negatively regulates NF-kappaB activation by facilitating selective autophagic degradation of IKKgamma. Nat Commun **8**, 2164 (2017).
28. Tabata M, *et al.* Angiopoietin-like Protein 2 Promotes Chronic Adipose Tissue Inflammation and Obesity-Related Systemic Insulin Resistance. Cell Metabolism **10**, 178–188 (2009).
29. Siddiqa A, Ahmad J, Ali A, Paracha RZ, Bibi Z, Aslam B. Structural characterization of ANGPTL8 (betatrophin) with its interacting partner lipoprotein lipase. Comput Biol Chem **61**, 210–220 (2016).
30. Deng B, *et al.* TAT-PEP Enhanced Neurobehavioral Functional Recovery by Facilitating Axonal Regeneration and Corticospinal Tract Projection After Stroke. Mol Neurobiol **55**, 652–667 (2018).
31. Bochner DN, *et al.* Blocking PirB up-regulates spines and functional synapses to unlock visual cortical plasticity and facilitate recovery from amblyopia. Sci Transl Med **6**, 258ra140 (2014).
32. Kazankov K, *et al.* The role of macrophages in nonalcoholic fatty liver disease and nonalcoholic steatohepatitis. Nat Rev Gastroenterol Hepatol **16**, 145–159 (2019).

33. Krenkel O, Tacke F. Macrophages in Nonalcoholic Fatty Liver Disease: A Role Model of Pathogenic Immunometabolism. Semin Liver Dis **37**, 189–197 (2017).
34. Navarro LA, *et al.* Arginase 2 deficiency results in spontaneous steatohepatitis: a novel link between innate immune activation and hepatic de novo lipogenesis. J Hepatol **62**, 412–420 (2015).
35. Stienstra R, *et al.* Kupffer cells promote hepatic steatosis via interleukin-1beta-dependent suppression of peroxisome proliferator-activated receptor alpha activity. Hepatology **51**, 511–522 (2010).
36. Miura K, Yang L, van Rooijen N, Ohnishi H, Seki E. Hepatic recruitment of macrophages promotes nonalcoholic steatohepatitis through CCR2. Am J Physiol Gastrointest Liver Physiol **302**, G1310-1321 (2012).
37. Zhang X, *et al.* CXC chemokine receptor 3 promotes steatohepatitis in mice through mediating inflammatory cytokines, macrophages and autophagy. J Hepatol **64**, 160–170 (2016).
38. Seki E, *et al.* CCR1 and CCR5 promote hepatic fibrosis in mice. J Clin Invest **119**, 1858–1870 (2009).
39. Zhang R. Lipasin, a novel nutritionally-regulated liver-enriched factor that regulates serum triglyceride levels. Biochemical and Biophysical Research Communications **424**, 786–792 (2012).
40. Kazankov K, *et al.* The macrophage activation marker sCD163 is associated with morphological disease stages in patients with non-alcoholic fatty liver disease. Liver Int **36**, 1549–1557 (2016).
41. Ohhira M, *et al.* Lipopolysaccharide induces adipose differentiation-related protein expression and lipid accumulation in the liver through inhibition of fatty acid oxidation in mice. Journal of Gastroenterology **42**, 969–978 (2007).
42. Odegaard JI, *et al.* Alternative M2 activation of Kupffer cells by PPARdelta ameliorates obesity-induced insulin resistance. Cell Metab **7**, 496–507 (2008).
43. Liao Z, *et al.* Angiopoietin-like protein 8 expression and association with extracellular matrix metabolism and inflammation during intervertebral disc degeneration. J Cell Mol Med **23**, 5737–5750 (2019).
44. Yang Y, *et al.* Increased Circulating Angiopoietin-Like Protein 8 Levels Are Associated with Thoracic Aortic Dissection and Higher Inflammatory Conditions. Cardiovasc Drugs Ther, (2020).
45. Jiao X, *et al.* Angiopoietin-like protein 8 accelerates atherosclerosis in ApoE(-/)(-) mice. Atherosclerosis **307**, 63–71 (2020).
46. Munitz A, *et al.* Paired immunoglobulin-like receptor B (PIR-B) negatively regulates macrophage activation in experimental colitis. Gastroenterology **139**, 530–541 (2010).

Figures

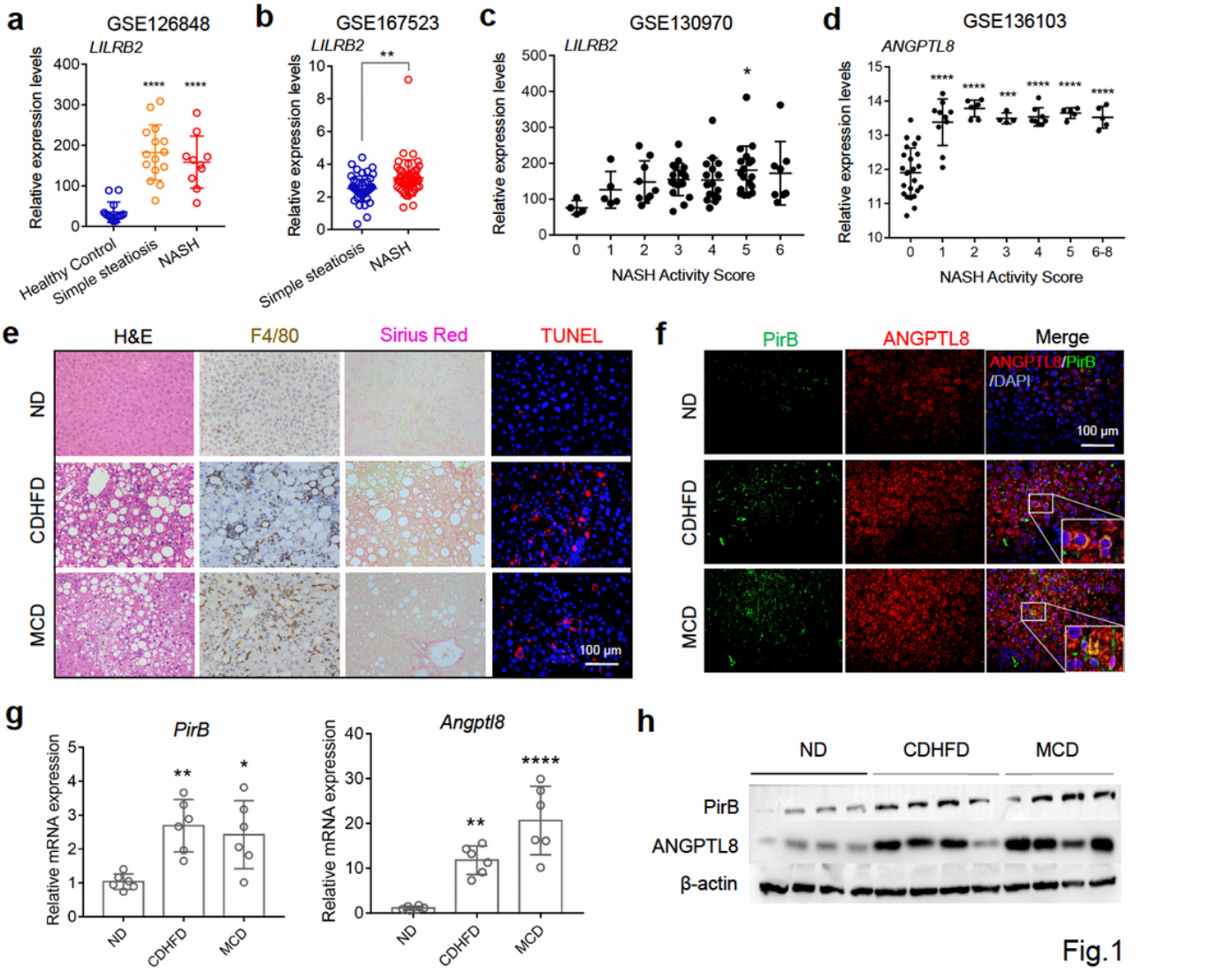

Figure 1

Increased ANGPTL8 and LILRB/PirB in the liver in human and murine NASH. (a-d) *LILRB2* and *ANGPTL8* mRNA levels in the livers of NASH patients from GEO datasets (GSE136103, GSE126848, GSE167523, and GSE130970). (d) NASH characterization by H&E, F4/80, Sirius Red, and TUNEL staining of the indicated groups. (e) Representative images showing immunofluorescence staining of PirB and ANGPTL8 in liver tissues. (f) Liver *PirB* and *Angptl8* mRNA expression in 6-month CDHFD-fed and 2-month MCD-fed mice. (g) Western blot analysis of liver ANGPTL8 and PirB protein in 6-month CDHFD-fed and 2-month MCD-fed mice. Scale bar, 100 μm. The data are shown as the mean ± s.e.m. (n = 5-7 mice/group) and were statistically analysed by one-way ANOVA with the Bonferroni test (a, c, d) or two-tailed Student's t test (b, g). *P < 0.05, **P < 0.01, ***P < 0.001, and ****P < 0.0001. ND: normal diet; CDHFD: choline-deficient high-fat diet; MCD, methionine-choline deficient.

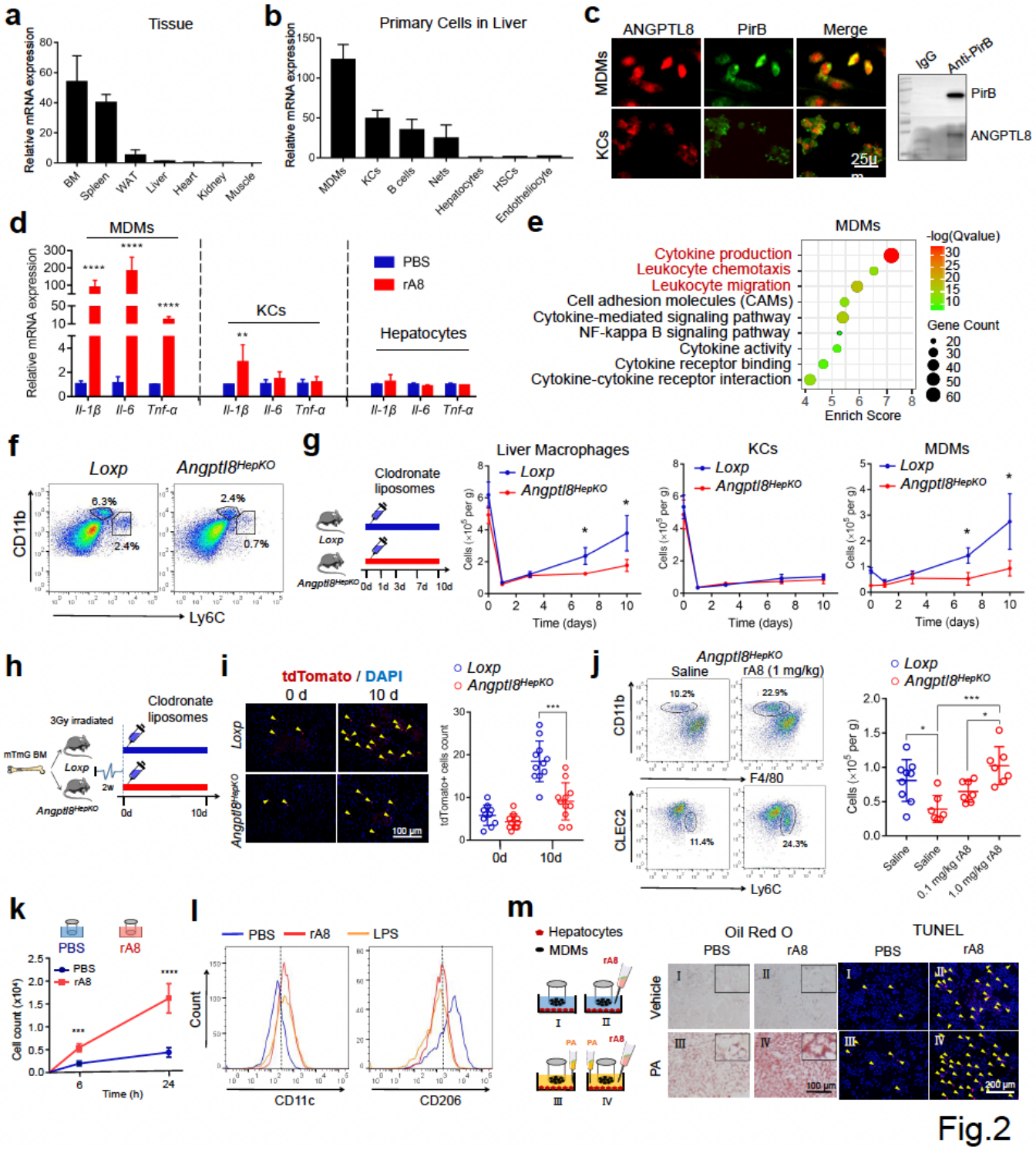

Figure 2

ANGPTL8 promotes MDM migration and activation. (a, b) *PirB* mRNA expression. (c) Immunocytochemistry staining to assess the colocalization of ANGPTL8 and PirB in hepatic macrophages (MDMs and KCs) treated with exogenous rA8. Scale bar, 25 μm. (d) Cytokine mRNA expression in MDMs, KCs, and hepatocytes treated with PBS and rA8. (e) Pathway enrichment analysis in MDMs treated with PBS and rA8. (f) Flow cytometry analysis of KCs (CLEC2^{hi} F4/80^{hi} CD11b^{lo}), MDMs (CLEC2^{lo}CD11b^{hi}F4/80^{lo}), and Ly-6C+ monocytes (CD11b^{hi} Ly-6C^{hi}) in *loxp/loxp* and *Angptl8^{HepKO}* mice.

(g) Liver macrophage, KC and MDM quantification in *loxp/loxp* and *Angptl8*^{HepKO} mice after KC deletion (0, 1, 3, 7, 10 days) with clodronate liposomes (n=3-4). (h) Experimental scheme to develop bone marrow (BM) chimaeras using *loxp* and *Angptl8*^{HepKO} cells as recipients and congenic mTmG cells as donors (n = 10-11). (i) tdTomato+ cells and quantification in liver sections. (j) Flow cytometry analysis of KCs (CLEC2^{hi}F4/80^{hi}CD11b^{lo}) and MDMs (CLEC2^{lo}CD11b^{hi}F4/80^{lo}) in the livers of *Angptl8*^{HepKO} mice after rA8 injection (n= 7-11). (k) Quantification of MDM migration to rA8 over time (n = 3-4). (l) Flow cytometry of MDM polarization after treatment with PBS (blue), rA8 (red), and LPS (orange). (m) Hepatocytes were cocultured with MDMs and treated with rA8 and PA, after which they were stained for lipid droplets (Oil Red O; scale bar, 100 μm) and apoptosis (TUNEL, highlighted by yellow arrow; scale bar, 200 μm). The data are shown as the mean ± s.e.m. and were statistically analyzed by one-way ANOVA (j) or two-tailed Student's t test (d, g, i, k). *P < 0.05, **P < 0.01, ***P < 0.001, and ****P < 0.0001. rA8, recombinant ANGPTL8 protein; KCs, Kupffer cells; MDMs, monocyte-derived macrophages; PA, palmitate.

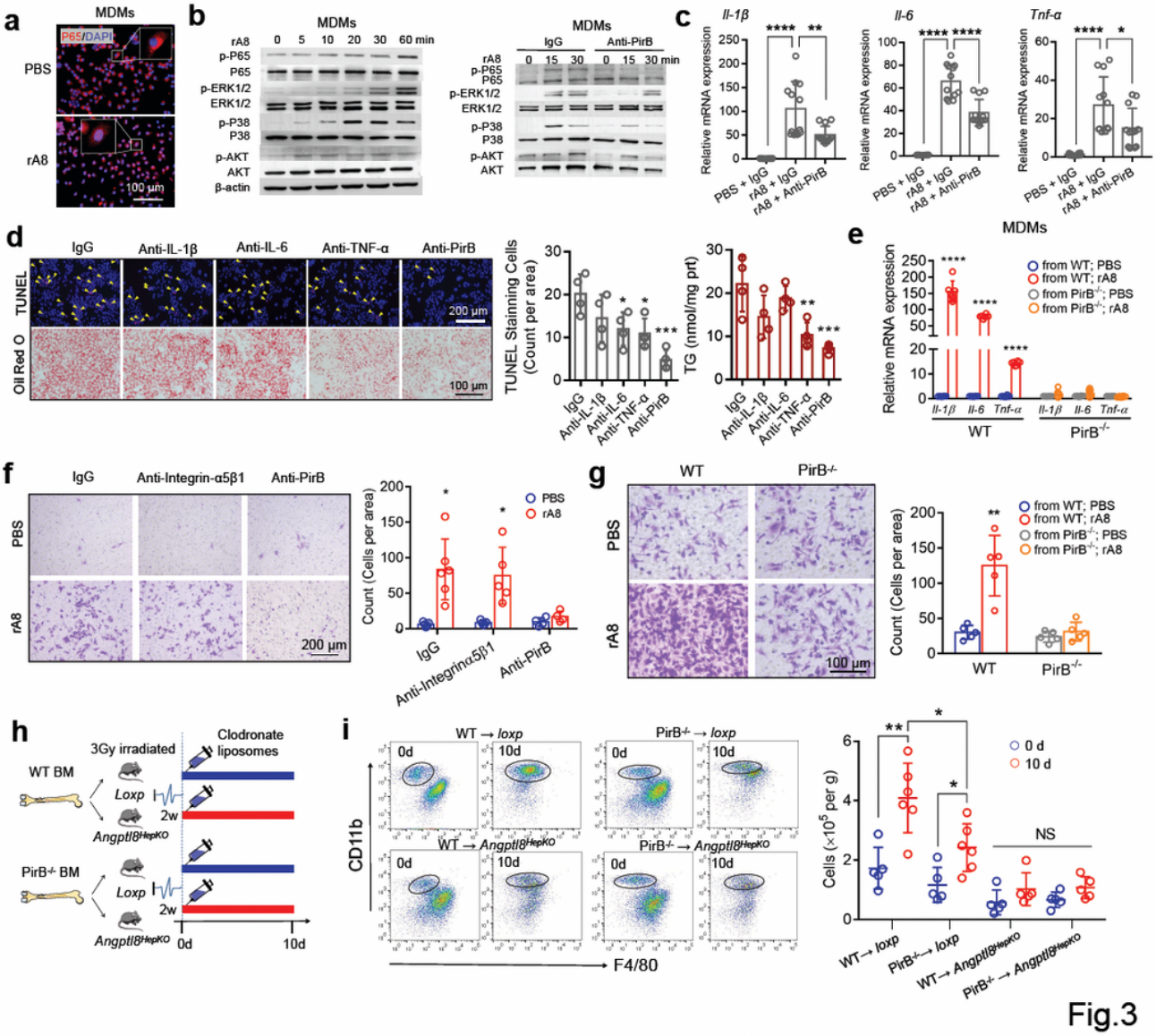

Fig.3

Figure 3

PirB mediates ANGPTL8-induced MDM migration and activation. (a) Nuclear translocation of P65 in MDMs. Scale bar, 100 μm. (b) Western blot analysis of the phosphorylation of signalling molecules downstream of PirB in MDMs treated with rA8 and anti-PirB antibody. (c) Effect of anti-PirB antibody on cytokine expression in rA8-treated MDMs (n = 12). (d) Effect of neutralizing antibodies against cytokines (anti-IL-1β, anti-IL-6, and anti-TNF-α) and PirB (anti-PirB) on lipogenesis and apoptosis of hepatocytes cocultured with MDMs in the presence of rA8 and PA (n = 4). (e) Cytokine expression of MDMs from WT or $PirB^{-/-}$ mice after rA8 or PBS treatment (n = 6). (f) Effect of anti-PirB antibody and anti-integrin-α5β1 on ANGPTL8-induced MDM migration (n = 4-6). Scale bar, 200 μm. (g) $PirB^{-/-}$ MDMs were resistant to ANGPTL8-induced migration (n = 5). (h) Experimental scheme to develop bone marrow (BM) chimaeras using *loxp* and $Angptl8^{HepKO}$ as recipients and WT or $PirB^{-/-}$ as donors. (i) Flow cytometry analysis and quantification of KCs ($CLEC2^{hi}F4/80^{hi}CD11b^{lo}$) and MDMs ($CLEC2^{lo}CD11b^{hi}F4/80^{lo}$, black circles indicated) in the livers of the indicated BM chimaeras (n = 5-6). The data are shown as the mean ± s.e.m. and were statistically analysed by one-way ANOVA (c and d) or two-tailed Student's t test (e-g and i). *P < 0.05, **P < 0.01, ***P < 0.001, and ****P < 0.0001. rA8, recombinant ANGPTL8 protein; KCs, Kupffer cells; MDMs, monocyte-derived macrophages; PA, palmitate; BM, bone marrow; NS, non-significant.

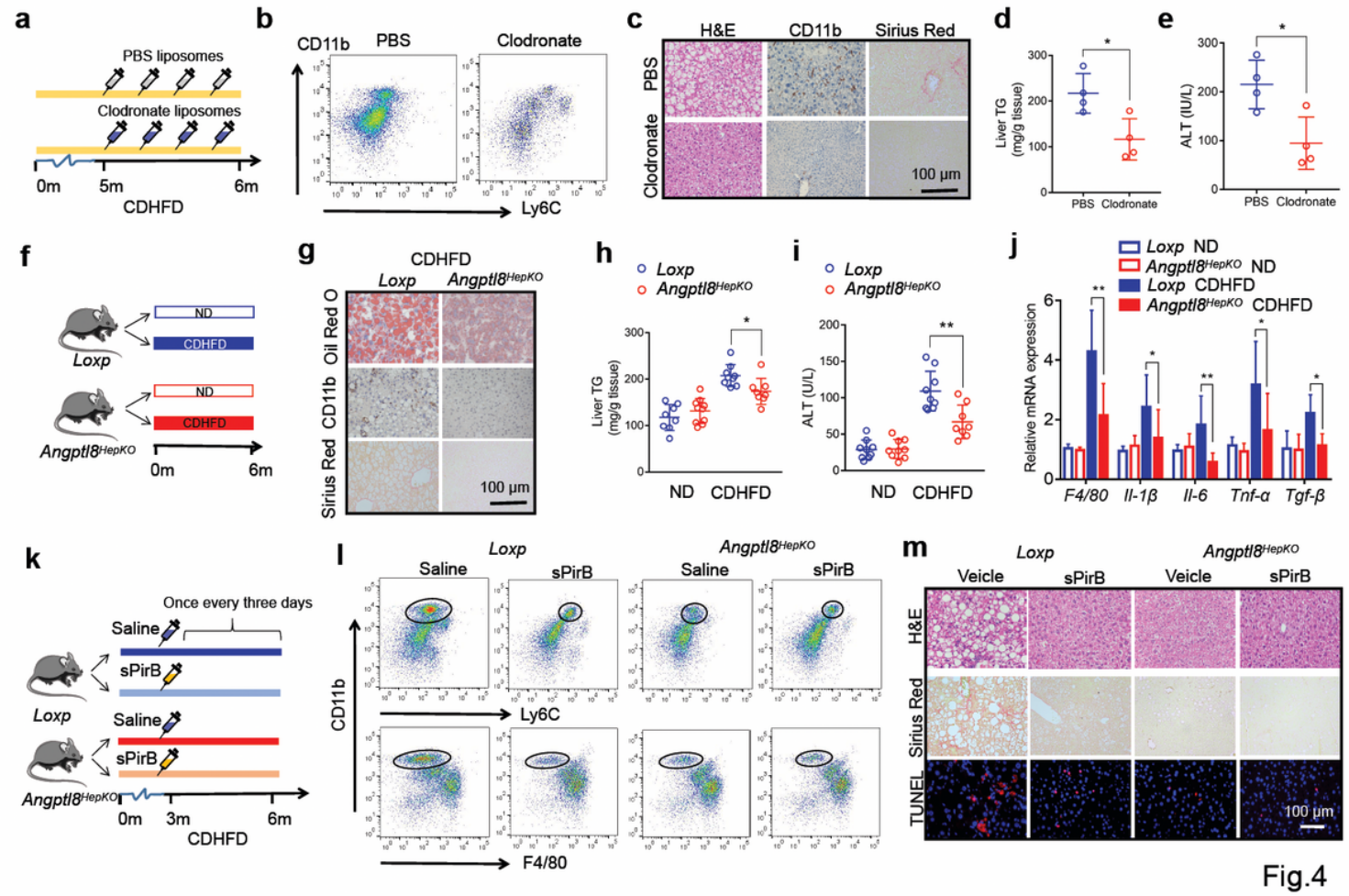

Fig.4

Figure 4

Hepatocyte-specific ANGPTL8 depletion and soluble PirB ectodomain (sPirB) protein ameliorate NASH. (a) Experimental setup for macrophage depletion in NASH livers. (b) Flow cytometry analysis of KCs and MDMs after macrophage deletion. (c) Representative liver images of liver sections. Scale bar, 100 μm. (d) Liver TG contents and (e) ALT of NASH mice with macrophage depletion (n = 4). (f) Experimental setup for inducing NASH in *Angptl8*^{HepKO} mice by CDHFD feeding. (g) Representative liver images of liver sections (scale bar, 100 μm), (h) liver TG contents, (i) ALT, and (j) inflammatory marker expression in the indicated groups. (k) Experimental setup for sPirB injection. (l) Flow cytometry analysis of KCs and MDMs 3 months after sPirB injection. (m) Representative liver images of liver sections. Scale bar, 100 μm. The data are shown as the mean ± s.e.m. and were statistically analysed by two-tailed Student's t test. *P < 0.05, **P < 0.01, ***P < 0.001, and ****P < 0.0001. MDMs, monocyte-derived macrophages, KCs: Kupffer cells; ND: normal diet; CDHFD: choline-deficient high-fat diet; sPirB, soluble PirB ectodomain protein.

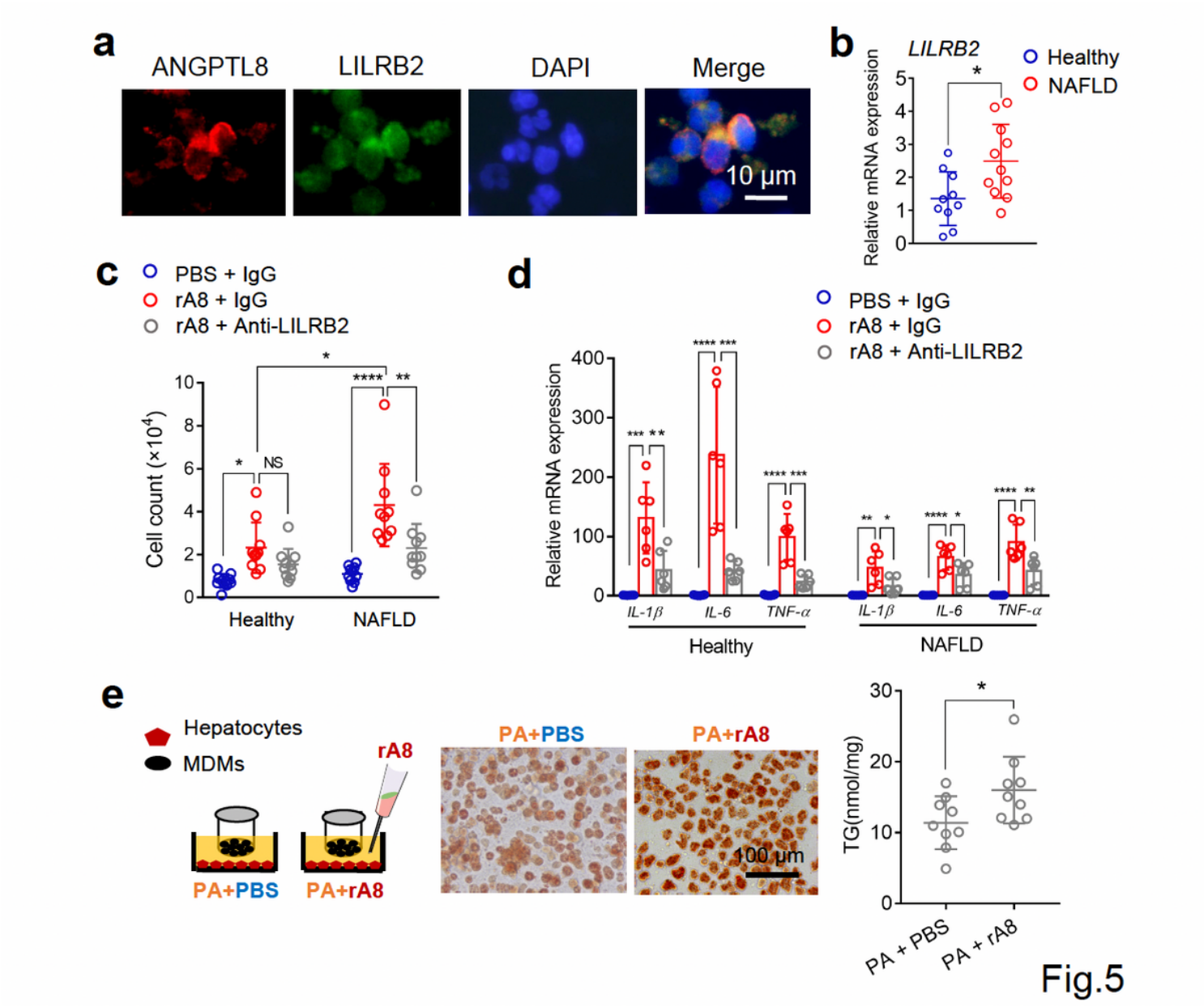

Figure 5

LILRB2 mediates ANGPTL8-induced human peripheral blood monocyte migration. (a) Immunocytochemistry colocalization of ANGPTL8 and LILRB2 on primary human peripheral blood monocytes (pHPBM) treated with exogenous rA8. Scale bar, 10 μm. (b) LILRB2 mRNA expression in pHPBMs from healthy adults and NASH patients (n = 10). (c) Migration of pHPBMs to ANGPTL8 was abrogated by anti-LILRB2 antibody (n = 10). (d) Cytokine mRNA expression in peripheral blood monocyte-derived macrophages treated with PBS and rA8 (n = 6). (e) Primary human hepatocytes were cocultured with monocyte-derived macrophages and treated with rA8 and PA, after which Oil Red O and TG were measured (scale bar, 100 μm). The data are shown as the mean ± s.e.m. and were statistically analysed by two-tailed Student's t test (b, d, e) and one-way ANOVA (c). *P < 0.05, **P < 0.01, ***P < 0.001, and ****P < 0.0001. pHPBM, primary human peripheral blood monocytes; rA8, recombinant ANGPTL8 protein.

Supplementary Files

This is a list of supplementary files associated with this preprint. Click to download.

- SupplementaryMethods.docx
- SupplementaryFigures.pdf
- SupplementaryTables.docx